Building a better unit cell: application to the Ag(111)/GaAs(110) system

2004 J. Phys.: Condens. Matter 16 4661

(http://iopscience.iop.org/0953-8984/16/26/002)

INSTITUTE OF PHYSICS PUBLISHING JOURNAL OF PHYSICS: CONDENSED MATTER

J. Phys.: Condens. Matter **16** (2004) 4661–4676 PII: S0953-8984(04)75052-3

Building a better unit cell: application to the Ag(111)/GaAs(110) system

Douglas L Irving[1], **Susan B Sinnott**[1,3] **and Richard F Wood**[2]

[1] Department of Materials Science and Engineering, University of Florida, 154 Rhines Hall, PO Box 116400, Gainesville, FL 32611-6400, USA
[2] Condensed Matter Sciences Division, Oak Ridge National Laboratory, Oak Ridge, TN 37831-6032, USA

E-mail: sinnott@mse.ufl.edu

Received 16 January 2004
Published 18 June 2004
Online at stacks.iop.org/JPhysCM/16/4661
doi:10.1088/0953-8984/16/26/002

Abstract

First-principles computational techniques are often employed in studies of heterogeneous material interfaces. In many cases the interface to be studied is not coherent or is only coherent over a small length scale and approximations to the unit cell are necessary to carry out the calculations. Instead of using large, computationally intractable unit cells, artificial strain is frequently induced into one or both of the materials making up the interface. This paper presents calculated adhesion energies for a variety of unit cells all chosen to model the Ag(111)/GaAs(110) interface. The results show that the calculated adhesion energy of a single monolayer of Ag is more dependent on the type of artificial strain introduced into the system than it is on the absolute magnitude of strain, and that the surface density of Ag within the monolayer is a crucial factor. The optimized surface structures are also analysed.

(Some figures in this article are in colour only in the electronic version)

1. Introduction

Heterogeneous material interfaces are a major area of research in both experimental and computational materials science. Understanding how two dissimilar materials interact at the interface is essential in most applications, but it becomes critical as the dimensionality of the material system is reduced to only a few monolayers. First-principles computational modelling is often used in conjunction with experiment [1–3] to better understand the interactions between two materials at a heterogeneous interface. However, this technique is often limited to a small number (∼100) of atoms.

[3] Author to whom any correspondence should be addressed.

Construction of a model that accurately and efficiently models the interface is then one of the major challenges in setting up a first-principles study. Often studies are performed on materials with drastically different lattice parameters, different crystal structures, and different crystal planes making up the interface. As a result, unit cells that achieve perfect coherence between the two materials or that capture the experimental misfit dislocation structures at the interface tend to be extremely large. To allow these systems to be modelled in first-principles calculations, larger unit cells with little or no strain must be approximated by smaller cells that may build considerable 'artificial' strain into one or both of the materials making up the interface. This paper analyses the consequences of introducing strain into the calculation of adhesion energy and surface structure of a one monolayer (ML) Ag(111) film on a GaAs(110) substrate.

Silver deposited onto GaAs(110) is non-wetting under normal deposition conditions and forms islands with tent like structures [4]. However, recent experiments have shown that flat Ag(111) layers can be grown by use of a two-step deposition process [5–7]. The first step of this process is to deposit the metal onto the GaAs substrate at about 100 K, which results in the formation of Ag nanoclusters. At this low temperature, the Ag atoms cannot diffuse readily on the surface and thus the nanoclusters cannot coalesce and grow, as they would at higher temperatures. This step is followed by a slow anneal to room temperature, which allows the Ag to coalesce and form the flat films observed in the experiments. Needless to say, the kinetic details of the process are not well known at this time.

The final morphology of the film is dependent not only on the temperature of deposition but also on the amount of Ag initially deposited. If an amount that is equivalent to less than 5 ML of Ag is deposited onto GaAs(110), then on annealing, islands of a uniform height of 15 Å form on the substrate. If the amount deposited is equivalent to 5 ML, atomically flat Ag(111) layers with occasional pinholes extending to the substrate form on annealing. Recent experimental studies indicate the smooth 5 ML films are metastable and will deteriorate over time [8]. From other studies, however, the authors [9] argue that deterioration only occurs in the presence of pinholes to the substrate, and that it occurs through a different mechanism than that of the initial stabilization. Finally, if an amount that is equivalent to more than 5 ML of Ag is initially deposited onto the substrate, a rough Ag film is formed on annealing.

Quantum size effects (QSE) are proposed as an explanation for the dependence of the annealed films morphology on coverage [10–13]. In [13], Zhang *et al* argue that itinerant electrons trapped between the metal/semiconductor interface and the metal/vacuum interface act to preferentially stabilize the metallic overlayers at particular thicknesses. The QSE are strong enough to overwhelm any true interfacial strain energy. They also assert that the calculated adhesion involved in adding a new layer of metal to the system can be used as a predictor for stability of that added layer. This claim is explored in simple calculations employing a free electron gas trapped between the vacuum level and a barrier at the metal-semiconductor interface in [13].

To date there has been only one attempt to use first-principles calculations to study the Ag(111)/GaAs(110) system. Sinnott *et al* [2] performed pseudopotential-based density functional theory (DFT) calculations on a 3D periodic slab of Ag(111)/GaAs(110). Due to computational limitations at the time, a small periodic interfacial unit cell was used that was obtained by straining the metallic layer(s) to achieve a coherent interface. Only one side of the 8 ML GaAs slab was covered with metal. In addition, during geometry optimization only the top three layers of any given structure were allowed to relax. The results for the adhesion energy as a function of the number of Ag layers were consistent with the trend predicted by the simple calculations of [13] up to 5 ML, but where the curve of Zhang *et al* continued asymptotically at the value reached for 5 ML, that of Sinnott *et al* rose sharply at that point.

Since this result clearly appears to be unphysical, the difference between the approximate and first-principles curves was tentatively attributed to the artificial strain built into the metallic layers due to the relatively small size of the periodic cell.

This paper analyses how induced strain effects the adhesion energy of a single ML of Ag on GaAs in a variety of unit cells of different sizes and with differing amounts of induced strain in the metallic overlayer. The calculations are a prelude to a much more extensive treatment of multilayer systems. From a computational standpoint, the Ag/GaAs system is quite complex, not only because of its structure but also because there is little experimental information about the orientation of the flat Ag overlayers with respect to the substrate. This fact emphasizes the need for a good deal of latitude in the creation of unit cells with differing amounts of strain. It will be shown that the magnitude of the strain in each system is less important than the type of strain (compressive or tensile) induced and the electron density at the interface. The strain-dependent effects on the morphologies of the various optimized Ag surface structure will also be analysed.

2. Computational details

Our study uses first-principles DFT [14, 15] in the CASTEP program [16–18] to calculate the ground state energies of the Ag(111)/GaAs(110) system. Pseudopotentials are used for each atomic centre, reducing the total computational cost of the calculation by self-consistently treating the valence electrons only. The valence electrons for the gallium atom include the $3d^{10}4s^{2}4p^{1}$ electrons in the self-consistent equation. The valence electrons included for As and Ag are $4s^{2}4p^{3}$ and $4d^{10}5s^{1}$, respectively. The norm-conserving pseudopotential of Lin [19] and the ultrasoft pseudopotential of Vanderbilt [20] are used in the calculations and comparisons are made between the results obtained using each. The norm-conserving pseudopotentials are projected in real space while the ultrasoft pseudopotentials are projected in reciprocal space. The electronic wavefunctions are expanded with a plane wave basis set up to a plane-wave cutoff energy sufficient for convergence, which varies depending on the convergence of each pseudopotential. The electronic energies are mapped to a set of special k-points in the reduced Brillouin zone and the number of k-points is determined by the spacing in the reciprocal space. A smaller k-point spacing yields a higher number of k-points and more accurate results, but it is also more computationally intensive. Initially, the default options for the k-point spacing are used as provided in the CASTEP software. Subsequently, a smaller k-point spacing is used for most of the unit cells without re-optimization of atomic positions within the cell. From the specified k-point spacing the k-point mesh can be determined by use of the Monkhorst–Pack generating scheme [21]. The exchange–correlation functional used in this study is the gradient corrected local density approximation of Perdew and Wang [22, 23], or GGA-PW91. Three-dimensional periodic boundary conditions are employed in all calculations with 27 Å of vacuum between each Ag–GaAs–Ag sequence.

Unless otherwise specified the following tolerances and values hold for all calculations. A kinetic energy cut off of 800 eV is used in conjunction with the norm-conserving pseudopotentials, while a cutoff of 340 eV is used with the ultrasoft pseudopotentials. In the case of electronic relaxation, the system energy is iterated until a tolerance 5×10^{-6} eV/atom is reached. For atomic relaxation, the forces on the atoms are minimized using the Broyden–Fletcher–Goldfarb–Shanno method [24] until the root mean-square (RMS) value is less than 0.1 eV Å^{-1} and the displacement RMS is less than 2.3×10^{-3} Å. The k-point spacing is 0.1 Å^{-1}. The total SCF energy change is 5×10^{-6}eV/atom and the energy between optimization steps is 5×10^{-5} eV/atom.

Table 1. The optimized lattice parameters for each pseudopotential in comparison to experiment.

Material	Ultrasoft lattice parameter (Å)	Norm-conserving lattice parameter (Å)	Experimental lattice parameter at 273 K [26] (Å)
GaAs	$a = b = c = 5.63$	$a = b = c = 5.71$	$a = b = c = 5.65$
Ag	$a = b = c = 4.13$	$a = b = c = 4.21$	$a = b = c = 4.09$

3. Construction of unit cells

The calculated bulk equilibrium lattice parameters depend on both the pseudopotentials and the defined tolerances. Because the focus of this study is to determine the effect of strain on the adhesion energy, it is imperative to minimize in the calculations any contributions to the strain not associated with the interface. Therefore, prior to building the heterogeneous interface unit cell, optimization of the bulk Ag and GaAs materials making up the interface is done for both pseudopotentials with exactly the same conditions that are to be used in the interface calculations. The results are shown in table 1.

After the bulk structures are optimized and the calculated bulk lattice parameters determined, the next challenge is to construct a model that accurately replicates the periodicity of both of the materials that make up the interface. As noted above, there is not much experimental information about how the flat overlayers orient themselves with respect to the substrate and this forced us to allow for a degree of rotational freedom in constructing the periodic cell. The near coincident site lattice (NCSL) method [25] is used to help find the appropriate scale lengths to replicate the heterogeneous system with our three-dimensional periodic boundary conditions. Once the GaAs(110) and Ag(111) slabs have been constructed, the next step is to align the surface normal of the two cleaved slabs with a common spatial axis. After alignment, the Ag is rotated about its surface normal until coincidence or near coincidence is found between a set of atomic positions in the metal layer and the substrate. Two possible orientations with small NCSL parameters were found for the Ag(111)/GaAs(110) system and these are shown in figure 1.

3.1. Orientation I

The first orientation is found by aligning the Ag(111) $[1\bar{1}0]$ and the GaAs(110) [001] directions and then the GaAs(110) $[\bar{1}10]$ and Ag(111) $[11\bar{2}]$ directions. A nearly strain free NCSL is produced. It spans one repeat unit in the GaAs(110) [001] direction, five repeat units in the GaAs(110) $[1\bar{1}0]$ direction, two repeat units in the Ag(111) $[1\bar{1}0]$ direction, and four repeat units in the Ag(111) $[11\bar{2}]$ direction. In other words, we form a 1×5 NCSL with reference to the GaAs substrate. All further NCSLs will be identified by the usual $m \times n$ notation, with m referring to the number of repeat units in the GaAs(110) [001] direction and n the number in the GaAs(110) $[\bar{1}10]$ direction. In the event of mismatch between the two structures, the artificial strain is built into the Ag layer only.

The nearly strain free 1×5 NCSL should be the ideal unit cell to use for both monolayer and multilayer calculations. However, as more Ag layers are added the total number of atoms involved becomes too large for practical purposes. From orientation I, we are also able to form two smaller NCSLs, the 1×4 and the 1×1. In the 1×4 and 1×1 unit cells the Ag(111) repeat distances in the $[1\bar{1}0]$ and $[11\bar{2}]$ directions are forced to match the scale lengths of the GaAs(110) substrate in the [001] and $[\bar{1}10]$ directions, respectively. In the 1×4 and 1×1 NCSLs there is little or no difference in the amount of induced strain in the Ag overlayer along the GaAs(110) [001] direction. However, along the GaAs(110) $[\bar{1}10]$ direction, three

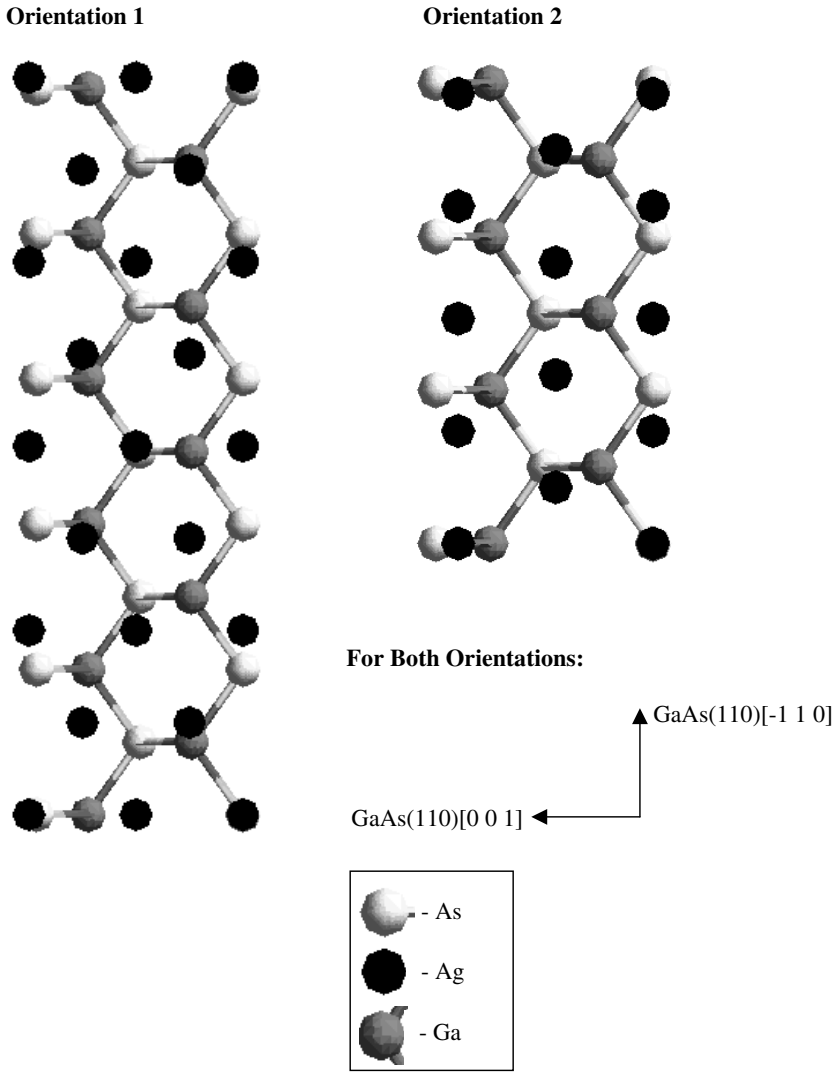

Figure 1. The two orientations of Ag(111) over GaAs(110) that are used in the construction of the heterogeneous unit cell are shown relative to specified orientation. See text for a description of the Ag(111) orientation with respect to GaAs(110) and the number of repeat units used to construct the periodic supercell. The black spheres represent the Ag atoms, the gray spheres represent the Ga atoms, and the white spheres represent the As atoms.

Ag repeat units are stretched to fit into the length of four GaAs repeat distances in the case of the 1×4 NCSL. In the case of the 1×1 NCSL, one Ag repeat distance is compressed to fit one GaAs repeat distance. Figure 1 illustrates these alignments. The 1×4 NCSL is slightly strained in comparison to the 1×5 while the 1×1 is the most strained of all the NCSLs coming from orientation I.

3.2. Orientation II

A second orientation for an NCSL is also found by first aligning the GaAs(110) [001] and the Ag(111) $[1\bar{2}1]$ directions, followed by alignment of the Ag(111) $[10\bar{1}]$ and GaAs(110) $[\bar{1}10]$

Table 2. Information on the induced strain in the unit cells and surface densities. A plus sign indicates tensile strain and a minus sign indicates compressive strain. Values can be compared to 13.83 Ag nm^{-2}, which is the surface density of the (111) plane of Ag with lattice parameters $a = b = c = 4.086$ Å. (US) denotes ultrasoft pseudopotential calculations and (NC) denotes calculations performed with norm conserving pseudopotentials.

Unit cell	Strain in Y (US) (%)	Strain in Z (US) (%)	Strain in Y (NC) (%)	Strain in Z (NC) (%)	Surface density (US) (Ag nm^{-2})	Surface density (NC) (Ag nm^{-2})
1×1	−21.21	−3.50	−21.76	−4.18	17.84	17.36
1×2	−9.02	11.43	−9.66	10.65	13.38	13.02
1×3	2.35	11.43	1.64	10.65	11.89	11.57
1×4	5.06	−3.50	4.32	−4.18	13.38	13.02
1×5	N/A	N/A	−2.20	−4.18	N/A	13.89

directions. From figure 1, it can be seen that a 1×2 and a 1×3 NCSL can be formed by compressing or stretching the Ag overlayer in a similar fashion as in the 1×1 and 1×4 unit cells of orientation I. For orientation II, one Ag repeat unit along the GaAs(110) [001] direction is stretched to fit one GaAs repeat unit. Along the GaAs(110) $[\bar{1}10]$ direction, three Ag repetitions are compressed to fit two in GaAs for the 1×2 unit cell. In the case of the 1×3 unit cell, four Ag units are strained in tension to match three of the GaAs repeat units. In other words the length scales of the Ag(111) layer are forced to match those of the GaAs(110) substrate for this new orientation.

These unit cells from the two orientations range from nearly matched to heavily strained. It is assumed that the strain in the unit cells is confined to the metallic layer due to the fact that metallic bonding is, in general, more forgiving of strain than is the bonding in an ionic or a covalent system. Table 2 summarizes the strain present in each interfacial unit cell. The strain is calculated in the Ag(111) $[1\bar{1}0]$ and Ag(111) $[11\bar{2}]$ directions for the 1×1, 1×4 and 1×5 unit cells and along the Ag (111) $[1\bar{2}1]$ and Ag(111) $[10\bar{1}]$ directions for the 1×2 and 1×3 NCSLs. These are the crystallographic directions for each unit cell that are forced to match the GaAs(110) [001] and GaAs(110) $[\bar{1}10]$ directions, respectively. For a given direction, the induced strain is defined by

$$S = 100 * (D_{\mathrm{f}}(\mathrm{Ag}) - D_{\mathrm{b}}(\mathrm{Ag}))/D_{\mathrm{b}}(\mathrm{Ag}). \tag{1}$$

$D_{\mathrm{f}}(\mathrm{Ag})$ is the forced repeat distance and $D_{\mathrm{b}}(\mathrm{Ag})$ is the calculated repeat distance in the bulk Ag. Positive and negative values of S mean tensile and compressive strains, respectively. Table 2 presents values for the induced strain as well as values for the surface densities of the Ag films created in this fashion.

Examples of the unit cells are shown in figure 2. The top views can be compared to figure 1, which shows the initial position of the Ag(111) layer over the GaAs(110) slab. From the side view it can be seen that there is a Ag(111) layer on each face of the GaAs slab, which is 5 ML thick. Due to the fact that there are three-dimensional periodic boundary conditions applied to these systems, several layers of vacuum must be added in the direction normal to the interface to isolate interfaces from one another. As mentioned above, the repeat distance from one surface to a surface in the next unit cell was initially 27 Å.

Once the unit cells are constructed, all the atoms in the system are allowed to relax through geometry optimization. Of course, the bulk unit cell parameters are held fixed at the values obtained from the earlier bulk optimization stage. There is some error associated with the optimization process due to the complicated task of finding the global minimum on a multi-dimensional potential surface. This is tested via multiple, nominally identical runs for the 1×2

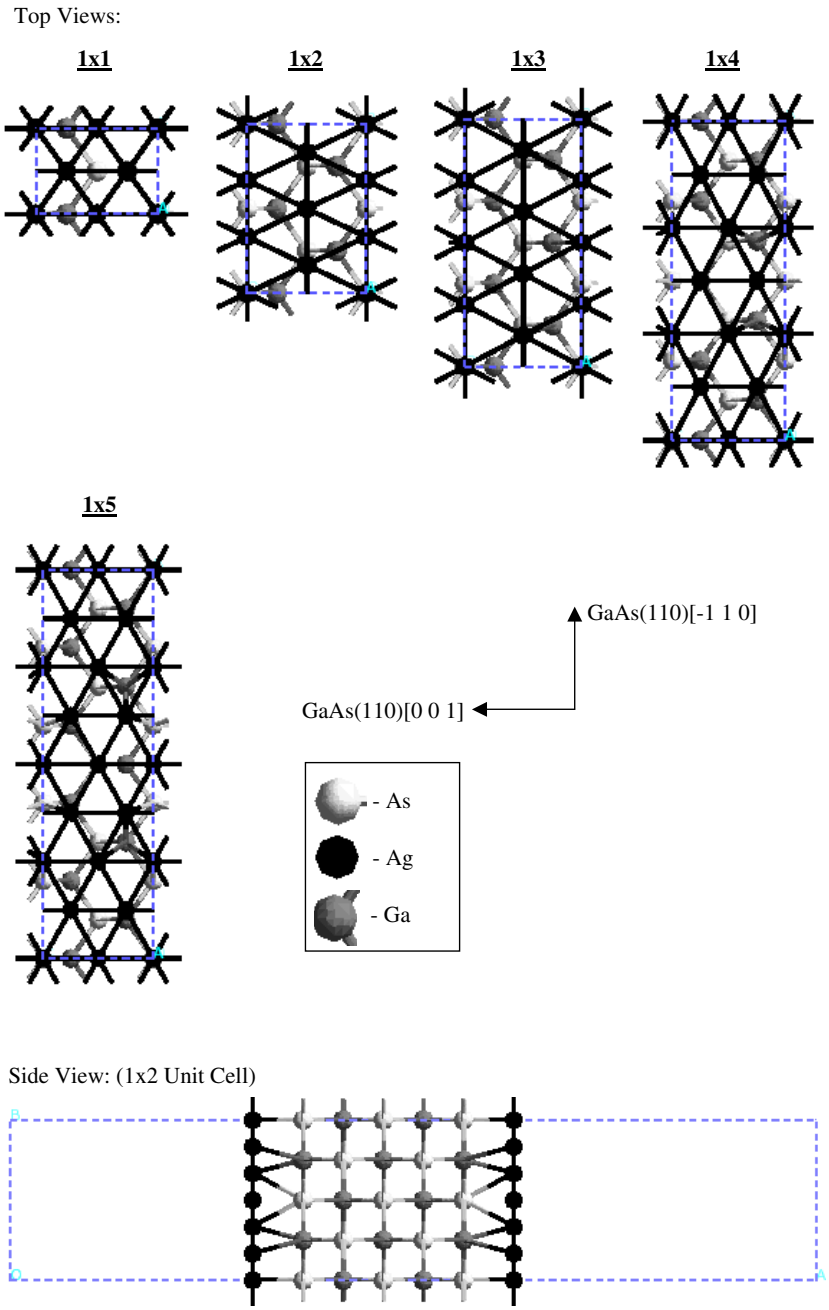

Figure 2. The five heterogeneous unit cells that are constructed from the orientations in figure 1 are presented here. The Ag overlayers in the cells range from very strained (1 × 1) to slightly strained (1 × 5).

NCSL using the ultrasoft pseudopotentials. The differences in the total energies of the relaxed structures range from 0.04 to 0.5 eV starting from the same initial positions. In the extreme case, this corresponds to a difference in the calculated adhesion energy of approximately 0.02 eV/Ag/interface for this unit cell.

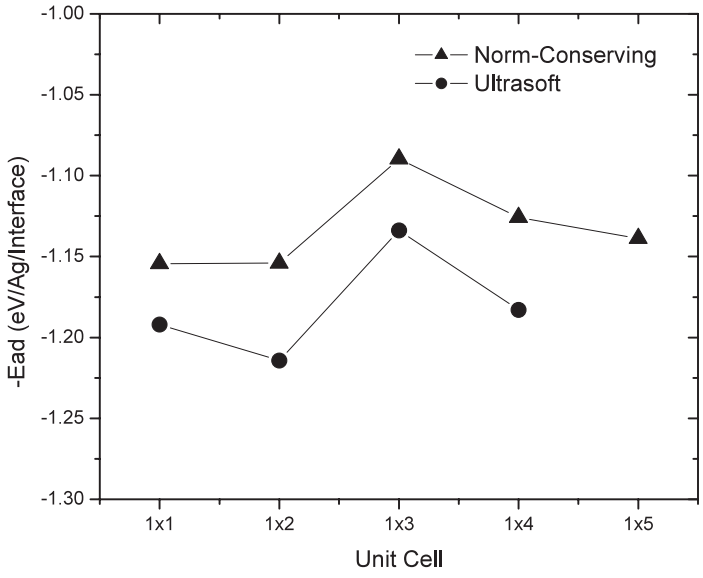

Figure 3. The calculated values for $-E_{ad}$ for the two pseudopotentials used are presented here. Both pseudopotentials show similar trends for the calculated adhesion energy from cell to cell.

4. Results and discussion

The energy needed to add a single layer of metal to the GaAs slab, which is one way of calculating adhesion energy, is determined from the total energy of the relaxed cells from the equation

$$-E_{ad}(n) = \frac{1}{2}\frac{(E(n) - E(n-1) - mE_{metal})}{m}. \tag{2}$$

In this expression $E(n)$ is the total energy of a relaxed unit cell with n layers of Ag, m is the total number of Ag atoms per layer, E_{metal} is the total energy of an isolated Ag atom and the factor of one half is included because there are two interfaces in each unit cell. It is important to note that the adhesion energy, E_{ad}, includes the cohesive energy of the Ag film when it is calculated in this fashion.

The values of $-E_{ad}$ for both pseudopotentials are plotted in figure 3 versus the unit cell used in the calculation. In each case, the system is a single layer of Ag(111) on the two faces of the five ML GaAs(110) slab. The figure shows that both pseudopotentials predict similar trends as one moves from the smallest unit cell (1×1) to the largest (1×5). The figure also indicates that the smallest absolute value of the adhesion energy is obtained for the 1×3 unit cell, while the largest values are predicted for the 1×1 and 1×2 unit cells.

Because systems of different sizes are being compared, it is necessary to make sure that there are no artifacts present in the calculation of the adhesion energy. One simple test of the numerical conditions used in the geometry optimization is to examine $E(0)$ for the various unit cells. This quantity is the total energy of the five-layer GaAs substrate and should be for all unit cells a multiple of the total energy of the 1×1 unit cell. Evaluation of $E(0)$ shows that the values for the optimized unit cells are not consistent in this regard and this is found to be due to the k-point spacing initially used in the various geometrical optimizations with the CASTEP defaults. In the optimizations three k-points are used for the 1×1 unit cell and one k-point is used for the 1×2 through 1×4 cells. The total energies of the relaxed GaAs slabs are subsequently recalculated without further optimization using a smaller k-point spacing of 0.05 $Å^{-1}$. This spacing generates 10, 6, 4 and 2 k-points for the 1×1–1×4 unit

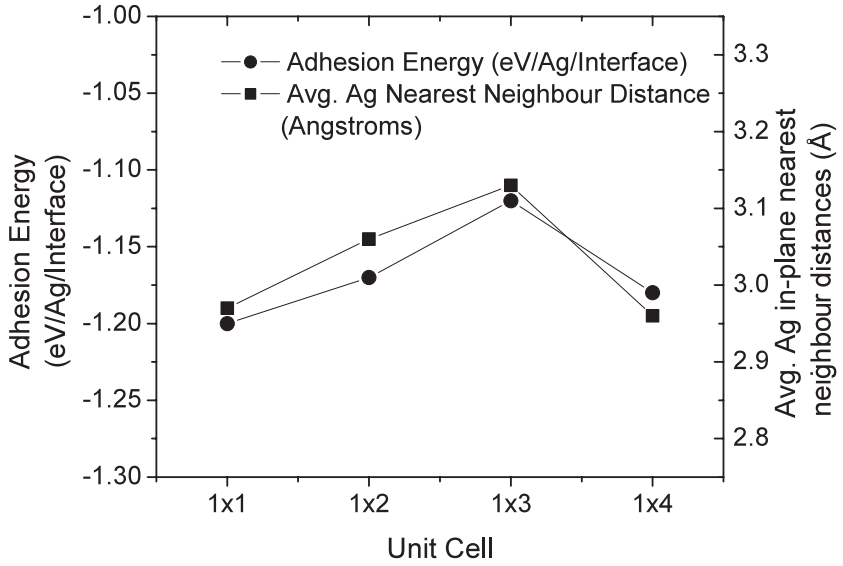

Figure 4. Plot of $-E_{ad}$ for ultrasoft pseudopotentials using the reduced k-point spacing. The Ag–Ag nearest neighbour distance is also plotted to show its relationship with the calculated adhesion energy.

cells, respectively. The RMS forces do not exceed $0.12\ \mathrm{eV/\AA^{-1}}$ in any of the GaAs unit cells. The normalized values for $E(0)$ are obtained by dividing the total $E(0)$ by the number of 1×1 unit cells that make up the larger unit cell.

The values for the normalized $E(0)$ are essentially constant when the k-point spacing is reduced, as expected. With the atomic positions held fixed at the values obtained from the optimized calculation, the total energy for each Ag/GaAs system was recalculated with the reduced k-point spacing of $0.05\ \mathrm{\AA^{-1}}$. The RMS forces in the monolayer calculations do not exceed $0.18\ \mathrm{eV/\AA^{-1}}$ with the change in k-point spacing. The values of the calculated adhesion energies are plotted for the reduced k-point spacing in figure 4.

The trend in the adhesion energy shown in figure 3 can be explained by the type (compressive or tensile) and magnitude of induced strain in the metal, the metal surface density and the average nearest neighbour distance around each Ag atom in the monolayer. These distances are calculated by taking the average distance of the six nearest Ag atoms in the plane around each atom centre. The nearest neighbour distances from the optimized cells are given in table 3. Figure 4 also shows a comparison between the trends in nearest neighbour distances to those of the adhesion energy. A strong correlation is seen between the two. The table shows that the 1×3 unit cell has the smallest absolute magnitude for the adhesion energy as well as the largest average nearest neighbour separation in the optimized Ag film. The 1×2 unit cell has the second smallest magnitude of the adhesion energy calculated with the finer k-point grid. The 1×4 and 1×1 unit cells have similar values, as well as similar nearest neighbour distances. This points to the importance of the lateral interactions of the Ag atoms in the calculation of the adhesion energy from equation (1).

Two additional calculations are performed in a further effort to establish the importance of the lateral Ag interactions in the calculation of the adhesion energy at the one ML level. Both calculations involve the 1×1 unit cell. The first starts with the optimized Ag/GaAs unit cell, which has by far the largest Ag surface density due to the compressions introduced

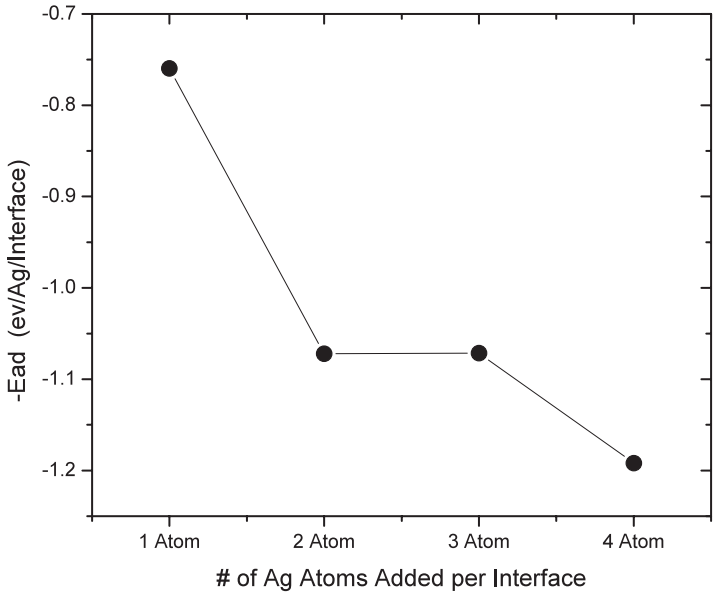

Figure 5. Plot of $-E_{\mathrm{ad}}$ as Ag atoms are added one at a time back to their optimized positions obtained in the ML calculation.

Table 3. Table of nearest neighbour distances, surface densities and adhesion energies.

Unit cell	Initial average N–N distance (Å)	Relaxed average N–N distance (Å)	Induced surface density (Ag nm^{-2})	$-E_{\mathrm{ad}}$ (k-point spacing = 0.05) (eV/Ag/interface)
1×1-I	2.57	2.97	17.84	−1.20
1×2	2.95	3.06	13.38	−1.17
1×3	3.12	3.13	11.89	−1.12
1×4	2.94	2.96	13.38	−1.18

during its construction. The interaction energy, E_{int}(Ag/GaAs), between a single Ag atom and the GaAs substrate as a function of the position of the Ag atom in the 1×1 unit cell has been mapped out previously in a lengthy series of calculations that will not be described here. All the Ag atoms are then removed from the GaAs substrate and replaced in their optimized positions one at a time in order of the E_{int}(Ag/GaAs) values, from largest to smallest. The total energy is calculated after each atom is added to the substrate and the adhesion energy or binding energy is determined from these energies. The results of this calculation are shown in figure 5. The results are remarkable because they show that the last-added Ag atom is, on its own, very weakly bound to the GaAs substrate, yet the adhesion energy increases dramatically when this atom is added. This atom is a part of the Ag film primarily because of the strong lateral interactions of the Ag atoms. This has implications that will be discussed further in the next section.

As can be seen from figure 5, the calculated absolute magnitude of the adhesion energy increases upon the addition of the second Ag atom. It remains approximately constant when the third Ag atom is added, but there is a marked increase as the fourth atom is added, as discussed above. We interpret this large increase as being due to the full delocalization of the electrons in the metallic overlayer. This delocalization has a major effect on the calculated adhesion energy because of the inclusion of the cohesive energy of the Ag layer in the definition of the adhesion energy in equation (2).

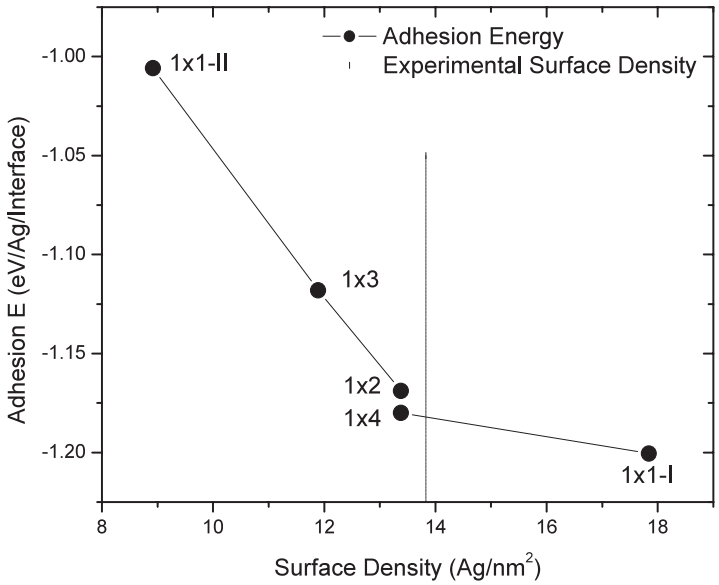

Figure 6. Plot of $-E_{ad}$ with the addition of the 1×1-II unit cell. The values of $-E_{ad}$ are plotted in order of surface density. In the case of equal surface densities values go from more strain to less strain.

These results are remarkable from another, but related, point of view. From table 3 it is seen that the adhesion energy for the 1 ML film is the greatest for the 1×1 unit cell and close to the value for the 1×4 cell. Also, the average nearest neighbour distances are very similar in the two unit cells. It is only in the Ag surface density that the two calculations show greatly different results. The Ag in the 1×1 cell is severely puckered while this is not the case in the 1×4 cell. Evidently, the Ag atoms adjust their positions to take advantage of the strong lateral Ag–Ag interactions at the expense of the weaker (at least for some atomic positions) Ag–GaAs interactions. Clearly, it is difficult to choose a satisfactory unit cell for a multilayer calculation based solely on the adhesion energy for the 1 ML calculations.

The second calculation that shows the importance of the Ag–Ag interactions involves creating a 1×1 unit cell from orientation II of figure 1. Here, this unit cell will be called 1×1-II and the original 1×1 unit cell discussed previously will be referred to as 1×1-I. When the Ag overlayer is forced to match the 1×1-II GaAs substrate, the Ag surface density is very low, approximately 8.92 Ag atoms nm^{-2}. The average distance to the six nearest neighbours after relaxation is also much larger than that for any of the previous unit cells and this cell is now the most extreme approximation for a ML of Ag. To be consistent with the procedure used above, the total energy of the optimized structure is also calculated using the k-point spacing of 0.05 Å^{-1}. The results of these calculations are shown in figure 6, which gives the adhesion energy of the system as a function of the increasing Ag surface density. Two unit cells, the 1×2 and 1×4, have identical surface densities but differing amounts of total strain. Figure 6 shows an increase in the magnitude of the adhesion energy with surface density, which again suggests the importance of the lateral interactions. From figure 6, the largest differences in the adhesion energy between the different unit cells occur for films that have a surface density that is too low, and nearest neighbour distances that are too small in comparison with the corresponding values for the Ag(111) plane.

The calculated adhesion energies using the reduced k-point spacing of the 1×1, 1×2 and 1×4 unit cells are very similar as shown in figure 4. There is a significant change to the 1×2 energy when the k-point spacing is decreased from the default value, as described above, which brought the calculated values of the energy of these three cells into close agreement.

The reduced k-point calculation gives a better estimate of the total energy of the bare GaAs slab, as discussed previously, and it is therefore assumed that this spacing also gives a better estimate of the adhesion energy. The 1×2 has the advantage of having a smaller number of atoms and would be a reasonable approximation of the heterogeneous unit cell as far as calculating the adhesion energy is concerned. This is the same unit cell orientation used by Sinnott *et al* in their original work with some subtle differences. The new unit cell has an Ag overlayer on both sides of the 5 ML GaAs slab, all atoms are allowed to relax, and the strain is distributed in a different fashion than in the previously used cell.

Although the effect of strain on the calculated adhesion energy is the primary focus of this study, induced strain also has a large effect on the morphology of the overlayer. For example, the Ag film in the 1×2 unit cell is stretched along the GaAs(110) [001] direction by 11.43% and compressed along the GaAs(110) [$\bar{1}$10] direction by 9.02%. The effect of having a large tensile strain can be seen from the top view of the optimized structure in figure 7. In the 1×2 cell, there are three columns of atoms aligned in parallel with the GaAs(110) [$\bar{1}$10] direction and they are separated by a larger distance than would normally be the case (i.e. in the bulk) in the GaAs(110) [001] direction. The first and third columns are periodic images of each other. In essence, if one moves then the other will move in the same fashion. This leaves the centre column to reduce the energy by moving closer to either column 1 or column 3. In the final structure the centre column strongly interacts with one of the columns and separates itself further from the other. This is also seen in the 1×3 and 1×1-II unit cells, which have the same orientation. Additionally, in the 1×2 there are four rows of Ag atoms parallel to the GaAs(110) [001] direction that are closer together than is energetically favourable. Because this plane is infinitely repeated by the supercell periodic boundary conditions, the only choice for movement to an energetically favourable distance during the optimization is for the Ag atoms to pucker out of the Ag(111)/GaAs(110) plane. This can be seen from the side view, showing the GaAs [110]–GaAs [$\bar{1}$10] plane, of the 1×2 unit cell where there is a large degree of puckering of the Ag layer.

The 1×4 has less strain built into it than does the 1×2. The Ag overlayer in the 1×4 is compressed in the GaAs(110) [001] direction by 3.50% and stretched in the GaAs(110) [$\bar{1}$10] direction by 5.06%. The five columns that align in parallel with the GaAs(110) [$\bar{1}$10] direction are only slightly too close together and from the top view it can be seen that there is minimal rearrangement of the original positions. The compressive strain along the GaAs(110) [001] direction is relieved by a slight puckering of the Ag, which can be seen in the view of the GaAs [110]–GaAs [001] plane of the 1×4 unit cell, as shown in figure 7. This method of relieving the induced strain is the same as seen in the 1×2 unit cell with a smaller amount of puckering due to the small amount of induced compressive strain. The side view of the GaAs [110]–GaAs [$\bar{1}$10] plane shows that in this case there is very little puckering of the 1×4 NCSL because of the small tensile strain of the Ag overlayer in the GaAs(110) [$\bar{1}$10] direction.

5. Conclusions

Induction of strain into the metallic layer in the Ag(111)/GaAs(110) system by the choice of the computational unit cell has effects on both the atomic structure and the calculated adhesion energy. The extent of the effects is dependent not only on the magnitude but also on the type of induced strain. This can be seen most clearly in the extreme examples of the two 1×1 unit cells. The Ag overlayer in the 1×1-I is initially compressed in both directions, but after optimization the monolayer of Ag atoms 'puckers' until the nearest neighbour distances are close to the bulk values. The magnitude of puckering in the 1×1-I cell is quite severe (the greatest of all the unit cells), yet the calculated value for the adhesion energy is very close

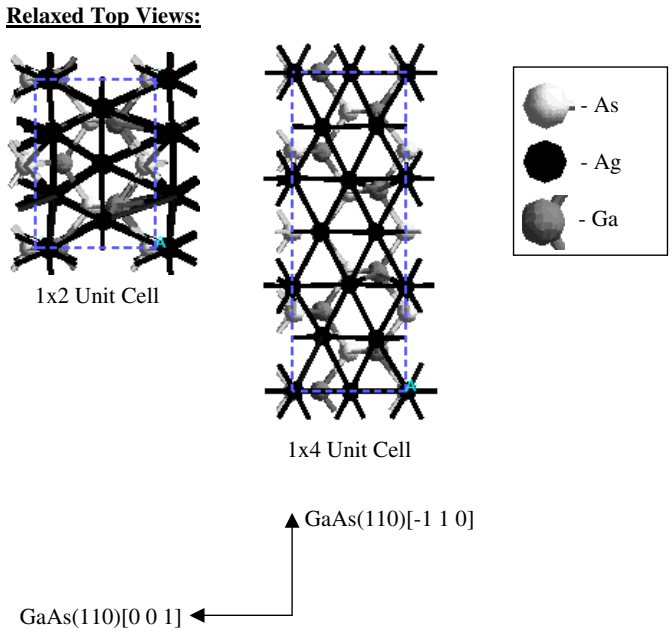

Figure 7. Comparison of the relaxed 1×2 and 1×4 unit cells. The top view of the 1×2 unit cell shows that the centre column of Ag atoms parallel to the GaAs(110) $[\bar{1}10]$ are forced to only significantly interact with one of the other two Ag columns. The 1×4 unit cell shows little rearrangement. The side view of both structures shows how induced strain effects puckering of the Ag overlayer.

to that of the slightly strained 1×4 and 1×5 unit cells. In contrast, the 1×1-II unit cell starts with an Ag overlayer that is stretched relative to the bulk in both directions. Because the Ag atoms are so far apart, there is no puckering even after geometrical optimization, but the adhesion energy is far different from that of the other unit cells; the Ag atoms are unable to move far enough to optimize their interaction. Illustrations of the 1×1 unit cells are provided in figure 8.

A good indication of whether or not a reliable value of the adhesion energy for films of true metals such as Ag and Au can be calculated with an approximate unit cell seems to be tied closely to the surface density of the films. Because of the lateral metal–metal interactions, when a film with the experimental surface density cannot be created it is better to have too many rather than too few atoms in the unit cell. However, as the compressive strain is increased, the surface structures of the overlayer become more puckered and probably less representative of structures observed experimentally. We note that the situation is quite different in the case of Sb on GaAs. Antimony is a semi-metal and the interfacial structure of a single ML is determined more by the overlayer-substrate bonding than by interactions within the overlayer.

When unit cells of different size are calculated with nominally identical conditions it is imperative to verify that those conditions actually do hold for all of the unit cells. As shown above, non-uniform $E(0)$ values are initially obtained due to too few k-points having been used to evaluate the energy during the geometry optimization. This problem is resolved by reducing the k-point spacing and re-evaluating the energy of the already relaxed structures. Forces are recalculated when this 'post-SCF optimization' was taken and all were reasonably small, so that further geometrical optimization is unnecessary.

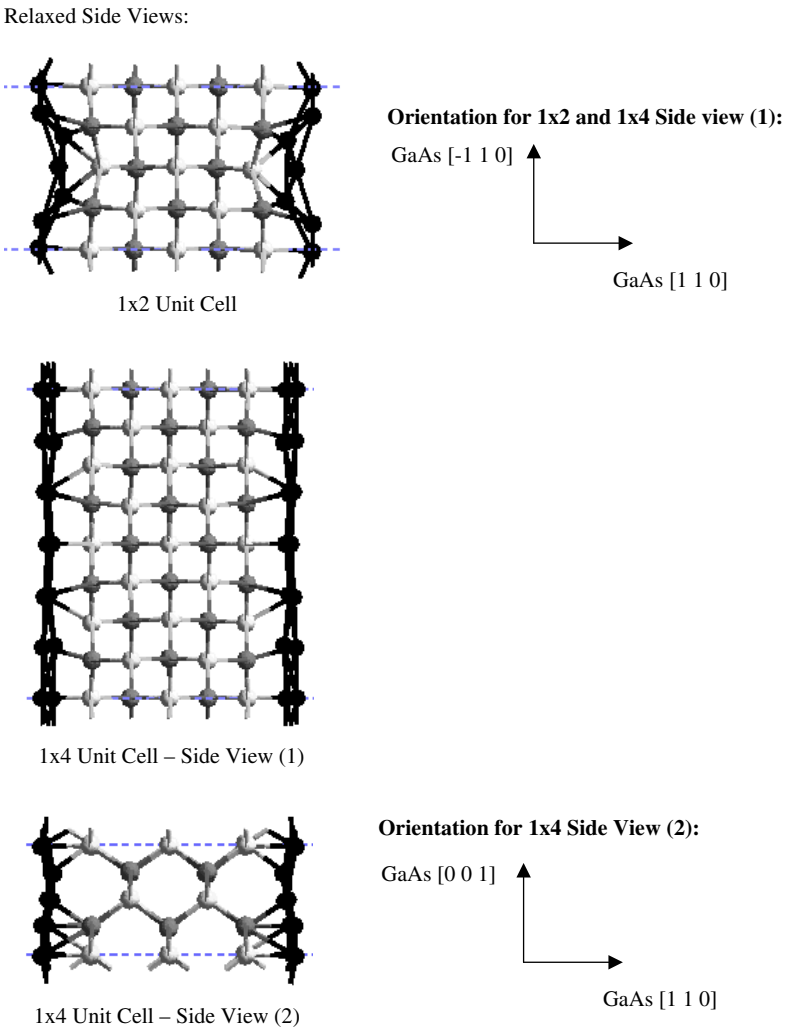

Figure 7. (Continued.)

We conclude that the results of our monolayer calculations reported here emphasize the importance of the Ag–Ag interactions for the morphology of the metallic film. While the Ag–GaAs interactions are quite important, they vary significantly over the atomic positions in the GaAs unit cell and, in fact, may be very small at some positions. Then at near-bulk Ag densities the Ag–Ag interactions largely determine the structure of the metal film. With these criteria in mind, it can be seen from table 2 that the 1×2 computational unit cell is a better choice than the 1×1 and the 1×3 cells. Both its Ag surface density and its adhesion energy are only marginally different from those of the 1×4 unit cell, and the density is only $\sim$3% less than the bulk density of the Ag(111) plane. Thus, the choice of the 1×2 cell in [2] was a good one at the time and remains so even now because the 1×4 and 1×5 cells are still computationally impractical when going to a multilayer (6–7 ML of Ag) calculation. The 1×3 calculation, which might be feasible, would probably give misleading results.

In a single monolayer calculation, nothing much can be said about quantum size effects in a direction perpendicular to the interface. However, the crucial role of the Ag–Ag interactions

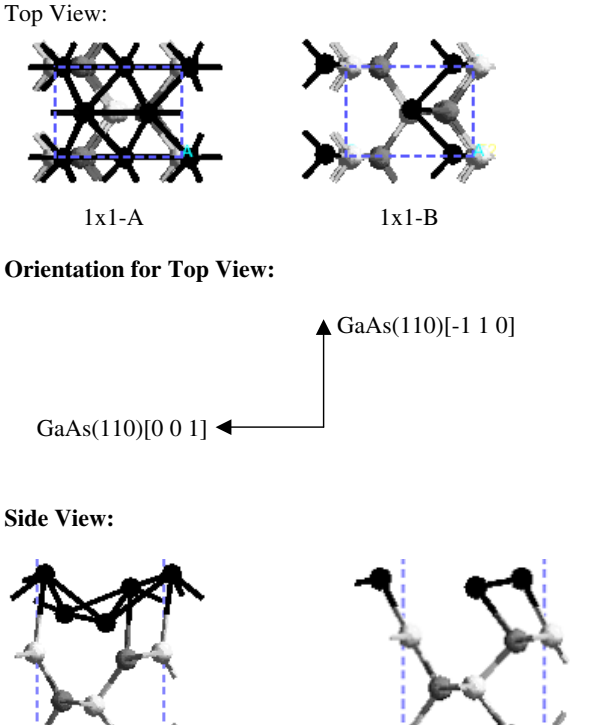

Figure 8. Comparison of 1×1-I and 1×1-II. Form the top view it can be seen that the 1×1-II unit cell relaxes in a similar fashion as the 1×2 in that the centre Ag atom interacts strongly with one column of atoms aligned with the GaAs(110) [$\bar{1}10$] direction. The side views again show the effect induced strain has on surface structures. Both 1×1 unit cells are extreme approximations for this interface.

does suggest that the system prefers to have the Ag at near-bulk values and with a coordination number approaching that of the bulk. It is not surprising then that a single monolayer is unstable against the tendency to form locally more bulk-like aggregates in which the QSE may become more apparent in first-principle calculations.

We note, however, that until the large jump of the calculated adhesion energy in the original calculation occurred, the behaviour of the adhesion energy in [2] with the number of layers is quite reasonable physically without introducing QSE. Also, since the extremely flat Ag films are now believed to be metastable, it may be difficult to justify a computation of their interfacial structure from ground-state first-principles calculations. Evidently a great deal of work remains to be done on the Ag/GaAs and similar systems.

Acknowledgments

The collaboration between DLI and SBS with RFW was initially facilitated by support through Southeastern Universities Research Association. We thank Zhenyu Zhang for many helpful discussions. This work was supported by the NSF grant DMR-9976851.

References

[1] Batyrev I G, Alavi A and Finnis M W 2000 Equilibrium and adhesion of Nb/sapphire: the effect of oxygen partial pressure *Phys. Rev.* B **62** 4698–706
[2] Sinnott S B *et al* 2000 Quantum size effects in metallic overlayer epitaxy *Japan. J. Appl. Phys.* **39** 4302–6
[3] Finnis M W 1996 The theory of metal–ceramic interfaces *J. Phys.: Condens. Matter* **8** 5811–36
[4] Trafas B M *et al* 1991 Scanning tunneling microscopy of Ag growth on GaAs(110) at 300-K-from clusters to crystallites *Phys. Rev.* B **43** 14107–14
[5] Smith A R *et al* 1996 Formation of atomically flat silver films on GaAs with a silver mean quasi periodicity *Science* **273** 226–8
[6] Neuhold G *et al* 1997 Thickness-dependent morphologies of thin Ag films on GaAs(110) as revealed by LEED and STM *Surf. Sci.* **376** 1–12
[7] Chao K J *et al* 1999 Substrate effects on the formation of flat Ag films on (110) surfaces of III–V compound semiconductors *Phys. Rev.* B **60** 4988–91
[8] Evans M M R, Han B Y and Weaver J H 2000 Ag films on GaAs(110): dewetting and void growth *Surf. Sci.* **465** 90–6
[9] Yu H B *et al* 2002 Quantitative determination of the metastability of flat Ag overlayers on GaAs(110) *Phys. Rev. Lett.* **8801** 016012
[10] Schulte F K 1976 Theory of thin metal-films–electron-density, potentials and work function *Surf. Sci.* **55** 427–44
[11] Feibelman P J 1983 Static quantum-size effects in thin crystalline, simple-metal films *Phys. Rev.* B **27** 1991–6
[12] Feibelman P J and Hamann D R 1984 Quantum-size effects in work-functions of freestanding and adsorbed thin metal-films *Phys. Rev.* B **29** 6463–7
[13] Zhang Z Y, Niu Q and Shih C K 1998 'Electronic growth' of metallic overlayers on semiconductor substrates *Phys. Rev. Lett.* **80** 5381–4
[14] Hohenberg P and Kohn W 1964 Inhomogeneous electron gas *Phys. Rev.* B **136** B864
[15] Kohn W and Sham L J 1965 Self-consistent equations including exchange and correlation effects *Phys. Rev.* **140** 1133
[16] Payne M C *et al* 1992 Iterative minimization techniques for ab initio total-energy calculations—molecular-dynamics and conjugate gradients *Rev. Mod. Phys.* **64** 1045–97
[17] Segall M D *et al* 2002 First-principles simulation: ideas, illustrations and the CASTEP code *J. Phys.: Condens. Matter* **14** 2717–44
[18] Milman V *et al* 2000 Electronic structure, properties, and phase stability of inorganic crystals: a pseudopotential plane-wave study *Int. J. Quantum Chem.* **77** 895–910
[19] Lin J S *et al* 1993 Optimized and transferable nonlocal separable ab initio pseudopotentials *Phys. Rev.* B **47** 4174–80
[20] Vanderbilt D 1990 Soft self-consistent pseudopotentials in a generalized eigenvalue formalism *Phys. Rev.* B **41** 7892–5
[21] Monkhorst H J and Pack J D 1976 Special points for Brillouin-zone integrations *Phys. Rev.* B **13** 5188–92
[22] Perdew J P and Yue W 1986 Accurate and simple density functional for the electronic exchange energy–generalized gradient approximation *Phys. Rev.* B **33** 8800–2
[23] Wang Y and Perdew J P 1991 Spin scaling of the electron-gas correlation-energy in the high-density limit *Phys. Rev.* B **43** 8911–6
[24] Press W H *et al* 1992 *Numerical Recipes in FORTRAN: the Art of Scientific Computing* 2nd edn (Cambridge: University of Cambridge)
[25] Wolf D and Yip S 1992 *Materials Interfaces: Atomic-Level Structure and Properties* (London: Chapman and Hall)
[26] Lide D R 1993 *CRC Handbook of Chemistry and Physics* 73rd edn (Boca Raton, FL: CRC Press)